water

MDPI

Article

Optical Properties of Dissolved Organic Matter and Controlling Factors in Dianchi Lake Waters

Min Xiao [1,*], Fengchang Wu [2], Yuanbi Yi [3], Zenglei Han [1] and Zhongliang Wang [1]

[1] Tianjin Key Laboratory of Water Resources and environment, Tianjin Normal University, Tianjin 300387, China; hanzenglei@tjnu.edu.cn (Z.H.); wangzhongliang@vip.skleg.cn (Z.W.)
[2] Chinese Research Academy of Environmental Sciences, Beijing 100012, China; Wufengchang@vip.skleg.cn
[3] Institute of Surface-Earth System Science, Tianjin University, Tianjin 300072, China; yuanbi.yi@tju.edu.cn
* Correspondence: xiaomin@vip.skleg.cn

Received: 14 August 2019; Accepted: 19 September 2019; Published: 21 September 2019

Abstract: Characterization of dissolved organic matter (DOM) is useful in understanding environment quality and carbon cycling in the lake system. In this study, the fluorescence of DOM, major ions, and nutrients in water were investigated to understand the sources and the transformation of DOM in Dianchi Lake, the sixth largest freshwater lake in China. The dissolved organic carbon content in water above the deposition layer was higher than 5 mg $C{\cdot}L^{-1}$ but lower than that in pore water. Two primary components of humic (C1) and protein-like components (C2) were identified using parallel factor (PARAFAC) modeling on sample fluorescence spectra. Organic components were related to mineral structures, and encapsulation of bacterial or algal cells into particulates could be disintegrated to release DOM. The aromaticity and the hydrophobicity of optical properties were regulated by percentages of chromophores (CDOM) of DOM in surface water, whereas by percentages of fluorophores (FDOM) in DOM in pore water, the underlying water layer was defined as a belt of transition. The molecular weight enhanced with percentages of C1 in CDOM increased in water above the sediment layer and the pore water at the northern lake site, but molecular weight attenuated with percentages decreased in pore water at the southern lake site. DOM not only originated from particulate decomposition but also derived from internal transformation among different, dissolved organic molecules. Small molecules were aggregated into larger ones, and, conversely, large molecules decomposed into small sizes. Another speculation is that dissolved molecules adsorbed or were encapsulated into particulates or were degraded and released into dissolved phases. The precise factors regulated composition, structure, and spectral properties of dissolved organic matter in the Dianchi Lake. This study highlights that sources of DOM and transformation mechanisms in the lake water could be correlated with nutrients and primary geochemical factors for mobility and distribution in different water compartments.

Keywords: dissolved organic matter; lake water; optical properties; fluorescence; transformation

1. Introduction

Dissolved organic matter (DOM) plays an important role in carbon biogeochemical cycling and the evolution of water quality in the aquatic system [1–3]. DOM generally derives from allochthonous (anthropogenic and terrestrial inputs) and autochthonal sources (microbial and phytoplankton) in the aquatic ecosystem [4–8]. In fact, dissolved organic matter decomposes into a set of different fractions and moieties whose reactivity and treatability can be entirely different from the bulk organic matter properties. Size, chemical composition, structure, and functional groups of DOM may vary greatly, depending on the origin and the age of the material [9–12]. Colored dissolved organic matter (CDOM) comprises 10–90% of the total DOM pool and therefore constitutes a significant

DOM fraction in aquatic ecosystems, controlling the photochemical reactions of the surface water and nutrient and light availability for aquatic organisms [11,13,14]. The transformations of DOM have been found to induce chemical interaction, cycling and production of inorganic carbon, nitrogen and phosphorus compounds, numerous low molecular weight organic compounds, as well as toxic chemicals throughout the environment [15,16]. During transformations of DOM, a detailed chemical and physical characterization of DOM is particularly useful for understanding the fate, the water properties, and the ecological effects in the aquatic environment.

With recent advances in spectroscopic techniques, ultraviolet-visible absorbance spectroscopy (UV-Vis) and fluorescence spectroscopy have become common organic matter (OM) characterization tools, providing rapid, non-invasive, and sensitive analysis of bulk OM properties [1,17]. Several spectral properties of the OM absorbance spectra have been proposed as surrogate parameters for characterization of OM reactivity and treatability, with specific ultraviolet absorption (SUVA) being the most commonly utilized. Absorption at 254 nm (or sometimes at 272 nm) has been widely used as an indicator of aromaticity and humification, and the absorption spectral slope ratio was used as an indicator of DOM from dissimilar water sources along the estuarine transect [18]. The reactivity difference of various waters or OM fractions with absorbance techniques could be discerned with difficulty. A series of optical indices for DOM quality can be measured by fluorescence excitation-emission matrices combined with parallel factor analysis (EEM-PARAFAC) [6]. Fluorescence spectroscopy could provide more useful information to understand the characterization of organic matter [19]. This, in turn, may improve our ability to predict the behavior of DOM and environmental pollutants in natural ecosystems. Molecular weight is a fundamental property of DOM and an important factor affecting the bioavailability of DOM [2]. Optical properties were also used to characterize water quality status and evolution [12].

A better understanding of the structural and the functional properties of DOM may greatly assist our further understanding of the underlying mechanisms responsible for the evolution of water environment quality, complexation, reduction, bioavailability, and mobilization/immobilization of elements with DOM [3,20,21]. Nutrients play an important role in the organic matter cycle, but which moiety in DOM is influenced has scarcely been investigated, as well as which fraction predominates or effectively changes bulk properties and structures [6,19–21]. Not much is known about biogeochemical transformation, composition, and nature alteration for DOM on horizontal and vertical watercourses in Dianchi Lake, Southwestern China. Dianchi Lake provides water resources for the local ecosystem as the sixth largest freshwater lake in China. Therefore, this study took Dianchi Lake as the studied area and mainly aimed to: (1) characterize the quality of DOM with absorption spectroscopy and fluorescence EEM-PARAFAC and confirm spectroscopic properties, source, and reactivity of DOM; (2) preliminarily understand the relevance of organic components to mineralogical elements and nutrients and examine the specific influence of microbial activity fed on nutrients and different DOM components (CDOM and different fluorescent components) in the Dianchi Lake.

2. Materials and Methods

2.1. Study Area

Dianchi Lake (24°40′–25°02′ N, 102°36′–102°47′ E) is a tectonic lake situated in the southwest of China, forming the middle part of Yunnan–Guizhou Plateau (Figure 1). It is a typical shallow plateau lake at an altitude of 1886.5 m, covering a watershed area of 2920 km^2 and a lake area of 309.5 km^2 and impoundage of 15.7×10^8 m^3. It has a mean depth of 4.7 m and a maximum depth of 11 m and a hydraulic retention time of 2.7 years [22]. Dianchi Lake is regarded as the sixth largest freshwater lake in China and the largest lake in Yunnan Plateau, which has a distinctive monsoon climate with an annual mean temperature of 15 °C, an annual mean precipitation of about 1000 mm, and an annual evaporation of 1870–2120 mm [23]. It provides water for industrial and agricultural production, regulation and storage, it contributes to flood prevention, travel, navigation, aquaculture,

etc., and it has been critical to national economic and social development in recent years. The inflowing rivers run through farmlands, cities, and grassland before reaching the lake. Dianchi Lake has faced increasing eutrophication and pollution, and its environmental status has become more fragile since the 1990s [24].

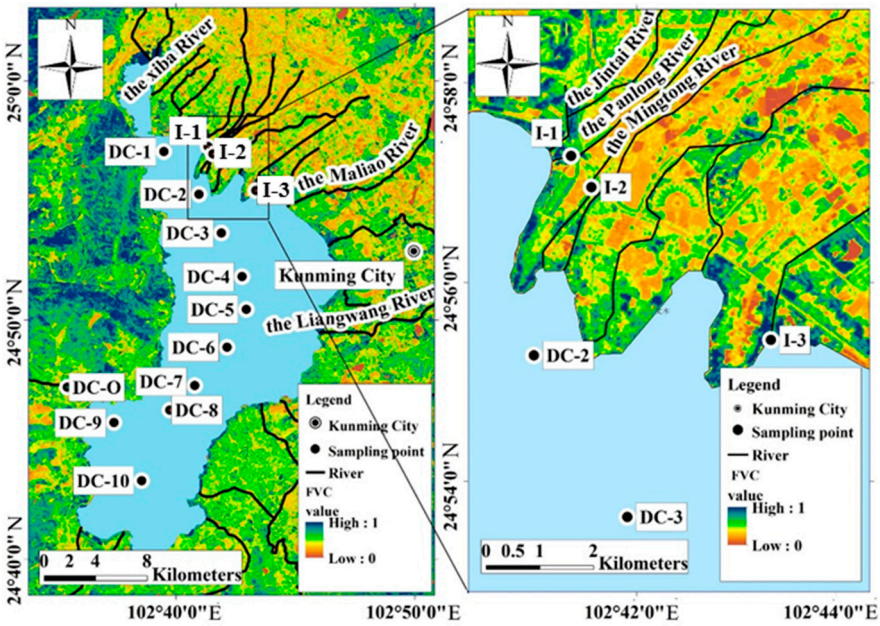

Figure 1. Location of Dianchi Lake in Yunnan Plateau and the sampling sites. FVC value: fractional vegetation cover value.

2.2. Sample Collection and Field Measurements

Surface water was sampled from the northern site, DC-1, to the southern site, DC-10, in the central water area, and a further three inlet sites (I-1, I-2, I-3) and one outlet site of DC-O were also sampled (Figure 1). Underlying water was restricted to a sample in the central water area from DC-1 to DC-10 sites. Sediments were sampled with a sediment cylindrical sampler to extract the solid core at DC-2 of the northern lake and DC-9 of the southern lake in the central lake area (Figure 1). Clean procedures were employed to avoid contamination, and all polyethylene sample bottles were acid washed (10% HNO_3 for 24 h) and rinsed with distilled water four times. Unfiltered water samples were analyzed for hydrochemical parameters such as temperature, pH, electrical conductivity (EC), total dissolved solids (TDS), and dissolved oxygen (DO), which were recorded with a portable meter (EXO1 Sonde, YSI company, Yellow Springs, OH, USA) on site. The parameters were calibrated with standard solutions before taking measurements.

The sediment–water interface was distinctly separated, and the cores were undisturbed during the sampling processes. The drill cores were sliced at 3 cm intervals above the 9 cm deposition column and thereafter by 5 cm as the slicing unit until deposition bottom at 49 cm. All samples were added to 50 mL centrifuge tubes, which were kept sealed and frozen. Lake water samples for geochemical analysis were filtered after sampling. A series of sediment samples were transported to the laboratory and centrifuged under 4000 rpm/min to extract pore water, and pore water was filtered using millipore Sterivex syringe capsules containing 0.45 µm cellulose acetate filters. The samples were then taken in polyethylene bottles, and samples were treated immediately after arrival at the laboratory to avoid potential alterations.

2.3. Analyses of Inorganic and Organic Compounds in Water and Porewater

Samples were transported to the laboratory for determination of dissolved organic carbon (DOC), anion and cation analysis. Determination of DOC was performed with a total organic carbon (TOC)

analyzer (Analytical Aurora 1030, OI Company, College Station, TX, USA). Ion chromatography (Dionex ICS-90 system, Thermo Scientific Company, Waltham, MA, USA) equipped with a 4 mm ASRS-ultra II suppressor and a DS-5 conductivity detector was used to measure anions, including nitrate (NO_3^-), sulfate (SO_4^{2-}), and chloride (Cl^-). HCO_3^- was measured by titration using methyl orange as the indicator. Measurements of silicates (SiO_3^{2-}), nitrites (NO_2^-), ammonium (NH_4^+), and phosphates (PO_4^{3-}) were performed on a Skarlar San++ continuous flow online analyzer (Skarlar Company, Breda, Netherlands). Cations Ca^{2+}, Mg^{2+}, Na^+, and K^+ were measured using an inductively coupled plasma optical emission spectrometer (ICP-OES, Agilent Company, Santa Clara, CA, USA). Quality control of the various detections was assessed with standard references, blank and duplicate samples, and the reproducibility of the analytical data was within 5%, and the analytical error was estimated to ≤10%.

UV-Vis absorbance spectra (200–600 nm, slit 0.5 nm, T9, Persee Company, Beijing, China) were recorded using a double beam UV-$T9_{CS}$ spectrophotometer on a 1 cm quartz cuvette, and the deionized water was used as reference solution. Specific UV absorbance at a wavelength of 254 nm ($SUVA_{254}$) was calculated as baseline-corrected absorbance at 254 nm relative to DOC concentration. The spectral slopes in the wavelength region 275–295 nm and 350–400 nm were determined by applying linear regression to natural log-transformed absorbance data in the corresponding wavelength region. $SUVA_{254}$ and $S_{350–400}/S_{275–295}$ corresponded to DOM aromaticity and the absorption spectral slope ratio (S_R) [16]. The fluorescence properties were measured using a fluorescence spectrophotometer (F-7000, Hitachi Company, Tokyo, Japan) with a 150 W ozone-free xenon arc lamp and a 1 cm quartz cell. The fluorescence spectra were collected at an excitation wavelength ranging from 220–400 at 5 nm increments and an emission wavelength ranging from 280–500 at 1 nm increments using a scanning speed of 1200 nm·min^{-1}. Deionized water from a Milli-Q instrument was measured as a blank. For normalization of fluorescence, quinine sulfate solution was used to calibrate fluorescence intensity. PARAFAC is a statistical tool that divides a large number of EEM datasets into several independent fluorescence components, separates the overlapping peaks, and objectively identifies characteristics and the relative content of each component. Parallel factor (PARAFAC) modeling is a three-way multivariate statistical analysis used extensively on EEM spectra to isolate and quantify the individual fluorescence component in terms of fluorescence intensity by decomposing the fluorescence matrices [25]. A two-component model was finally chosen for this study, as indicated by the second-highest core consistency (99.9%) and a relatively higher explained variance (90.8%). The relative concentration of each PARAFAC component was estimated by the F_{max} value from DOM fluorescence. The fluorescence index (FI) is effective to discern the source of DOM [26]. The Pearson correlation coefficient and the one-way analysis of variance (ANOVA) were performed using statistical package software (SPSS, version 19, IBM Company, New York, NY, USA).

3. Results and Discussion

3.1. Characterization of Water Chemistry and DOC in the Dianchi Lake Waters

The temperature in the pore water was 17.3 °C, 2.8 °C higher than average values in surface water. The water above the deposition layer was weakly basic with pH ranging from 7.12~9.07 and a narrower range of 7.24~8.48 in pore water. The conductivity value averaged 365.3 at DC-2 and 374.9 μS·cm^{-1} at DC-9, which was 55.1 μS·cm^{-1} higher in pore water than that in the water above the deposition layer. Total dissolved solids (TDS = [Ca^{2+} + Mg^{2+} + Na^+ + K^+] + [HCO_3^- + SO_4^{2-} + Cl^-]) ranged from 236 to 448 (average 263.29) and 240 to 247 (average 242.7) mg·L^{-1} in surface and underlying water, respectively, and this index was not measured in pore water. The percentage contribution of Ca^{2+} and Na^+ in cations was more than 69%, while Mg^{2+} and K^+ was lower. The ion balance of total cations and anions (meq·L^{-1}) was better than ±5%.

Nitrate concentrations were high, ranging from 1.47 to 44.64 mg·L^{-1} in samples of surface and underlying water and 1.04 to 80.14 mg·L^{-1} in pore water. NO_3^--N was of 1.9 mg·L^{-1} in surface water and close to water quality standard value listed as class V of 2 mg·L^{-1} for total nitrogen [27], indicating

that the water quality in Dianchi Lake was deteriorating. Bicarbonates (HCO_3^-) concentration ranged from 94.54 to 220.59 and 87.01 to 116.7 mg·L^{-1} in surface and underlying water, respectively. The Dianchi Lake water could be defined as HCO_3-Ca type due to relatively high Ca concentration in total cations [28]. SO_4^{2-} concentrations in surface and underlying water were 24.27 to 50.54 and 43.19 to 51.77 mg·L^{-1}, respectively, which did not differentiate as much as that in pore water, where it ranged from 5.46 to 29.42 and 6.94 to 40.55 mg·L^{-1} in the pore water of DC-2 and DC-9, respectively. The ratio Ca/Mg represented salinity and acidity/alkalinity in a paleoenvironment, which exhibited concordant variant trends with HCO_3^- in water compartments above the sediments in this study, with the average values of 2.61 and 1.94 in the pore water and the water above the deposition layer.

DOC in surface water ranged from 1.59 to 6.24 mg C·L^{-1}, and the lowest value was at the inlet river water of DC-1. This basically fluctuated around 5.84 mg C·L^{-1} in the central water area. DOCs were 5.25 and 5.55 mg C·L^{-1} in water above the deposition layer but only 4.43 mg C·L^{-1} at DC-2 and 3.81 mg C·L^{-1} at DC-9 for the pore water. Organic matter can provide physical sites for metal adsorption and electron donors for sulfate reduction [29]. DOCs were experienced identically with SO_4^{2-} ($R^2 = 0.98$, $p \leq 0.01$) in that both of them were the same sources or experienced the same geochemical processes, i.e., along with disintegration of the bound carbonatite and halide minerals and at much lower levels at inlets than at the lake central region. Almost all of the anions were HCO_3^- and Cl^-, which might have been due to bedrock and minerals weathering and anthropogenic inputs around the lake drainage area [27,28]. This resulted from SO_4^{2-} being utilized as an electron acceptor to oxidize DOM, during which HCO_3^- and SiO_3^{2-} were produced from organic phases. Due to a large amount of anthropogenic discharge [27], NO_3^- was 32.84 mg·L^{-1}, much higher at inlets than that of 2.24 mg·L^{-1} found at the central lake region. It was utilized as an electron acceptor during DOC mineralization, and this only happened in the central water areas DC-1 to DC-10. HCO_3^- and pH were the highest and the lowest at inlets, corresponding to 3.11 mmol·L^{-1} and 7.38. EC and TDS were also highest with 454.13 μS·cm^{-1} and 346.67 mg·L^{-1}, respectively, at those sites.

3.2. Sources of DOM Based on Spectral and Fluorescent Characteristics

The parameter of *a* (355) represented the UV-absorption coefficient at 355 nm, an index for the content of CDOM [30]. Its values ranged from 1.38 to 3.92 m^{-1} in water above the deposition layer and from 1.38 to 4.15 m^{-1} in the pore water. Fluorescent dissolved organic matter (FDOM) ranged from 27.47 to 116.61 quinine sulphate units (QSU) in water above the deposition layer and 70.06 to 115.51 QSU in the pore water. It was more abundant in the pore water and, at 38.09 QSU, it was higher than the water above the deposition layer. C1 and C2 were generally higher in pore water at DC-2–53.70 and 43.82 QSU, respectively. The lower S_R values explained the higher molecular weight of DOM at inlets. They were 1.40 and 0.92 on average in waters above the deposition layer, and in the pore water, the trough value of 0.51 presented at I-3. Previous studies used SUVA at 254 nm as a proxy for DOM aromaticity as it is strongly correlated with percentage aromaticity determined by ^{13}C NMR [18]. $SUVA_{254}$ indicates aromaticity of terrigenous origination, and SUV260 denotes the hydrophobicity of DOM, averaged as 2.83 and 2.73 L·(mg C)$^{-1}m^{-1}$ and 5.28 and 4.64 L·(mg C)$^{-1}m^{-1}$ in the above mentioned two parts of the water. The values of fluorescence intensity, humification (HIX), and biological (BIX) indices ranged from 1.91, 2.10, 1.15 to 2.06, 2.47, and 1.18 in lake water, respectively (Table 1).

The fluorescence images of surface, underlying, and sediment pore water in Dianchi Lake are presented in Figure 2. In water compartments, the fluorescence index averaged 1.9 or exceeded 2.0, suggesting that autochthonous OM was predominant for suspended particulates from authigenic micro-organic residues and algal excretion/detritus decomposition. High BIX values (>1) and low HIX values (<4) connected to autochthonous DOM [31]. BIX ranged from 1.04 to 1.23 and a HIX range from 1.71 to 4.14 ordinarily fluctuated around 2.13 except for the only extreme value 4.14 at I-1, further illustrating the predominantly autochthonous origin of DOM and occasionally allochthonous origin in surface waters.

Table 1. Spectral and fluorescent properties of dissolved organic matter (DOM) in surface, underlying, and pore water.

Station	DOC mg C·L^{-1}	FDOM QSU	CDOM m^{-1}	C1	C2	C1/FDOM	C1/CDOM QSU·m	C2/CDOM QSU·m	$SUVA_{254}$ Lm^{-1} (mg C)$^{-1}$	$SUVA_{260}$ Lm^{-1} (mg C)$^{-1}$	FI	HIX	BIX
I-1	1.59	27.47	1.38	16.17	11.30	0.59	11.72	8.18	4.92	4.63	1.87	4.14	1.04
I-2	3.43	87.24	2.30	41.49	45.75	0.48	18.02	19.86	4.03	4.03	2.09	2.12	1.18
I-3	4.35	116.61	3.45	50.92	65.69	0.44	14.76	19.04	3.97	3.71	2.07	1.76	1.23
DC-O	5.98	48.61	2.99	24.53	24.07	0.50	8.19	8.04	2.70	2.54	1.88	1.95	1.18
SW	5.25	53.12	2.48	26.47	26.65	0.51	10.79	10.63	3.00	2.83	1.91	2.10	1.18
UW	5.55	46.12	2.46	23.80	22.32	0.52	10.01	9.33	2.60	2.58	1.90	1.96	1.18
DC-2	4.40	98.52	2.97	54.70	43.82	0.56	19.99	15.61	5.50	4.89	2.06	2.47	1.15
DC-9	3.81	78.98	1.94	41.19	37.79	0.53	23.25	21.05	5.08	4.41	2.06	2.19	1.17

I: denotes inlets of lake; DC-O: outlet of lake; SW: surface water; UW: underlying water; DC-2, DC-9: pore waters; DOC: dissolved organic carbon; FDOM: fluorescent dissolved organic matter; CDOM: colored dissolved organic matter; SUVA: specific ultraviolet absorption; FI: fluorescent intensity; HIX: humification index; BIX: biological index; QSU: quinine sulphate units.

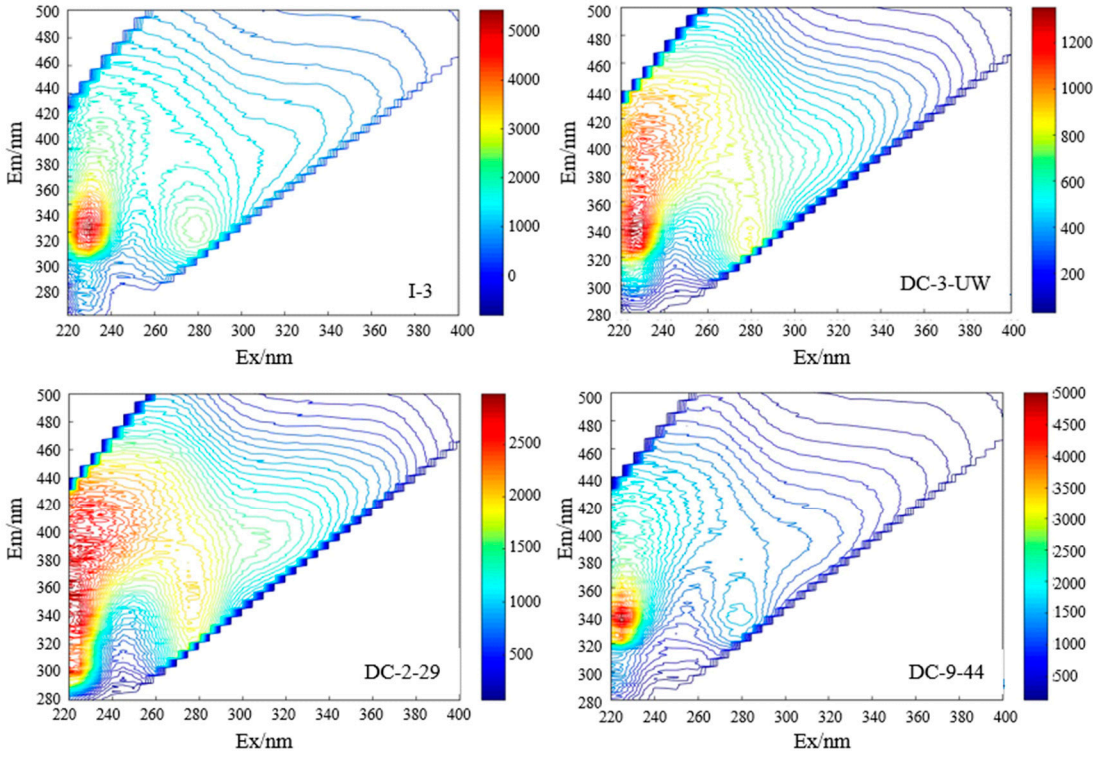

Figure 2. Examples of the fluorescence spectra of surface, underlying, and sediment pore waters collected from Dianchi Lake in different sampling points. I-3: third inlet river (Figure 1); DC-3-UW: underlying water of DC-3 site; DC-2-29: water from 29 cm in the sediment of DC-2; DC-9-44: water from 44 cm in the sediment of DC-9; Ex: excitation wavelength; Em: emission wavelength.

For this study, the DOC/FDOM/CDOM normalized Fmax values (F/DOC) and the percentage abundance of each component (%C1 and %C2) were included as PARAFAC indicators. Component 1 showed three fluorescence peaks (Ex/Em pairs at 250/440 nm; 315/440 nm; and 315/410 nm). Peaks at 250/440 nm and 315/440 nm were similar to the traditional terrestrial humic-like peak A and peak C [32], and spectral features were also similar to other reported terrestrial humic-like matter. These two short wavelength (UV and visible spectrum) humic-like peaks originated from fulvic-like substances [33,34]. This fraction of fluorophores were more hydrophobic, larger in molecular unit, and non-biodegradable [35]. Peak M was a typical humic-like fluorescence that was observed originally in productive oceanic environments but now has been found in freshwater impacted by agriculture [36]. The fluorescence images of fluorescent components in the water compartments of Dianchi Lake are presented in Figure 3. Component 2 showed two fluorescence Ex/Em maxima such as peak Tuv at Ex/Em = 225/341 as the strong peak with high fluorescence intensity, whereas peak T at Ex/Em = 275/341 was shown as a minor peak with low fluorescence intensity. This component corresponded to a protein-like substance tryptophan with two fluorescence peaks at ultraviolet and visible regions [37]. Component 2 (Ex/Em = 225/341 and 275/341) came from highly proteinaceous material. Protein-like substances with autochthonous sources were easily adsorbed onto the sediment minerals and/or retained by the microorganisms on the sediments [38,39]. It was suggested that humic-like components originated from microbial/algal activities, having probably been associated with a more condensed structure and larger molecular size and a relatively more refractory nature, whereas the tryptophan-like C2 fluorophore was less structurally condensed and more labile [34]. The highest FDOM appeared in pore water DC-2 by 98.52 QSU. C1 and C2 nearly accounted for 50% of FDOM in surface and underlying water, respectively, but C2 was slightly higher in pore water than that in water above the deposition layer. The percentage of C1 in FDOM was always anti-correlated with that of C2, which indicated that these two components mutually transformed in the above mentioned water

compartments. FDOM also accounted for the highest proportion in DOC in pore water at DC-2 by 25.3 L·QSU·(mg C)$^{-1}$. Whatever the FDOM or the percentages of FDOM in DOC were, the values were both higher in pore water than in water above the deposition layer, e.g., they merely averaged 46.1 QSU and 8.33 L·QSU·(mg C)$^{-1}$ in underlying waters. Fluorescence intensity of humic acid decreased with decreasing molecular weight and pH and increasing ionic strength [40]. It was the same phenomenon for molecular weight with pH values in surface water at Dianchi Lake but with converse ionic strength. Proportions of humic-like DOM increased with ionic strength increasing, both reaching the highest at inlets with 12.1 L·QSU·(mg C)$^{-1}$ and 0.01 mol·L^{-1}. The above correlations between humic-like DOM and molecular weight, pH, and ionic strength were not observed in the underlying and the pore water. The humic-like organic matter was a major source for DOM in Dianchi Lake.

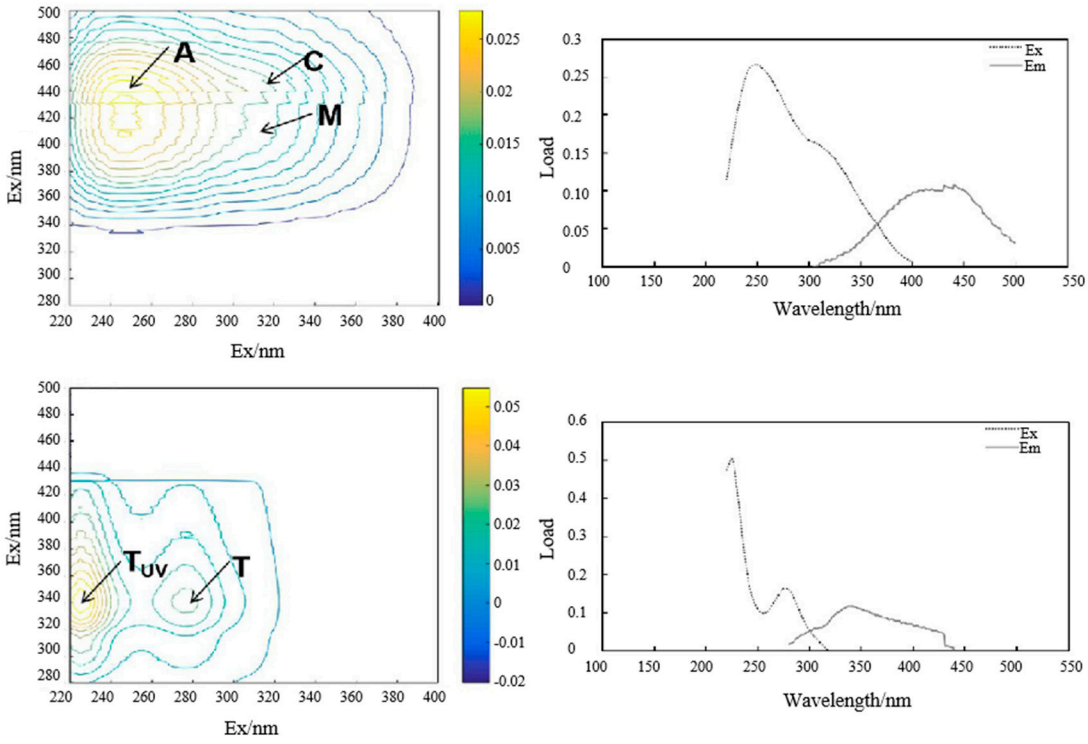

Figure 3. Fluorescent components in the water compartments of Dianchi Lake. On the left: spectral properties of DOM from the two sediments obtained by the parallel factor analysis (PARAFAC). Lines represent the loadings from the two-component model using the whole dataset. A: humic-like component in violet region; C: humic-like component in visible region; M: humic-like component related to microbial origination; T: protein-like component in visible region; Tuv: protein-like component in violet region; Ex: excitation wavelength; Em: emission wavelength; The blue-yellow column represents fluorescent intensity after PARAFAC calculation. Arrows point to the peak of components. On the left: changing load of DOM components along with increasing wavelengths after PARAFAC calculation.

3.3. Analysis of Relationship between Water Chemistry and Characteristic of DOM in Dianchi Lake Waters

Dissolved organic carbon in water could be produced from the disruption or the disintegration of organomineral complexes and could decrease binding of humic acid (HA) or fulvic acid (FA) by metal oxides, osmotic shock, and lysis of microbial cells [3,11,41]. Therefore, part of DOC resulted from bedrock mineralization and erosion along with the degradation of OM by microbial cells, and this kind of collapse effect was most evident at inlets. The total fluorescent intensity in surface waters was highest at inlets with 137.69 QSU. Nutrients such as N, P, and Si accumulated at inlets; they had the same horizontal trends with total FDOM ($R^2 = 0.87$, $P \leq 0.01$), indicating that they all originated from the disintegration and the degradation of particle encapsulation of organic matter into mineral structures. This opinion was verified from the obvious positive correlations between FDOM and

HCO_3^-, Ca^{2+}, Na^+, K^+ (R^2 = 0.95, P ≤ 0.01), ratios of Ca/Mg and Na/K (R^2 = 0.94, P ≤ 0.01), and a significant negative correlation between FDOM, pH, and DO (R^2 = −0.66, P ≤ 0.01). Other than release from mineral lattice, the fluorescence effect of DOM could be intensified by an increase of Ca^{2+} and Mg^{2+} [19,42].

Ratios of Ca/Mg consistently fluctuated around 1.64 from DC-1 to DC-10 in the central lake (Figure 4) but reached up to 4.09 abruptly at lake inlets. Higher water alkalinity resulted from particulate and dissolved organic matter anaerobically decomposing in surface water, producing HCO_3^- and H^+ that both behaved identically. Organic matter (particulate and dissolved organic matter) was degraded anaerobically the most at lake inlets, where pH and DO values dropped to their lowest at 7.13 and 2.98 mg·L^{-1}. FDOM was concentrated rapidly at inlets and was thereafter basically unchanged and fluctuated around 56.43 QSU in the central lake region. FDOM/CDOM indicated the ratio of intensity of florescent DOM to that of chlorophore DOM [6,12,19]. The ratios of FDOM/CDOM in lake inlets and surface water were generally lower than those in pore water, suggesting that humification plays an important role in DOM transformation in the sediments.

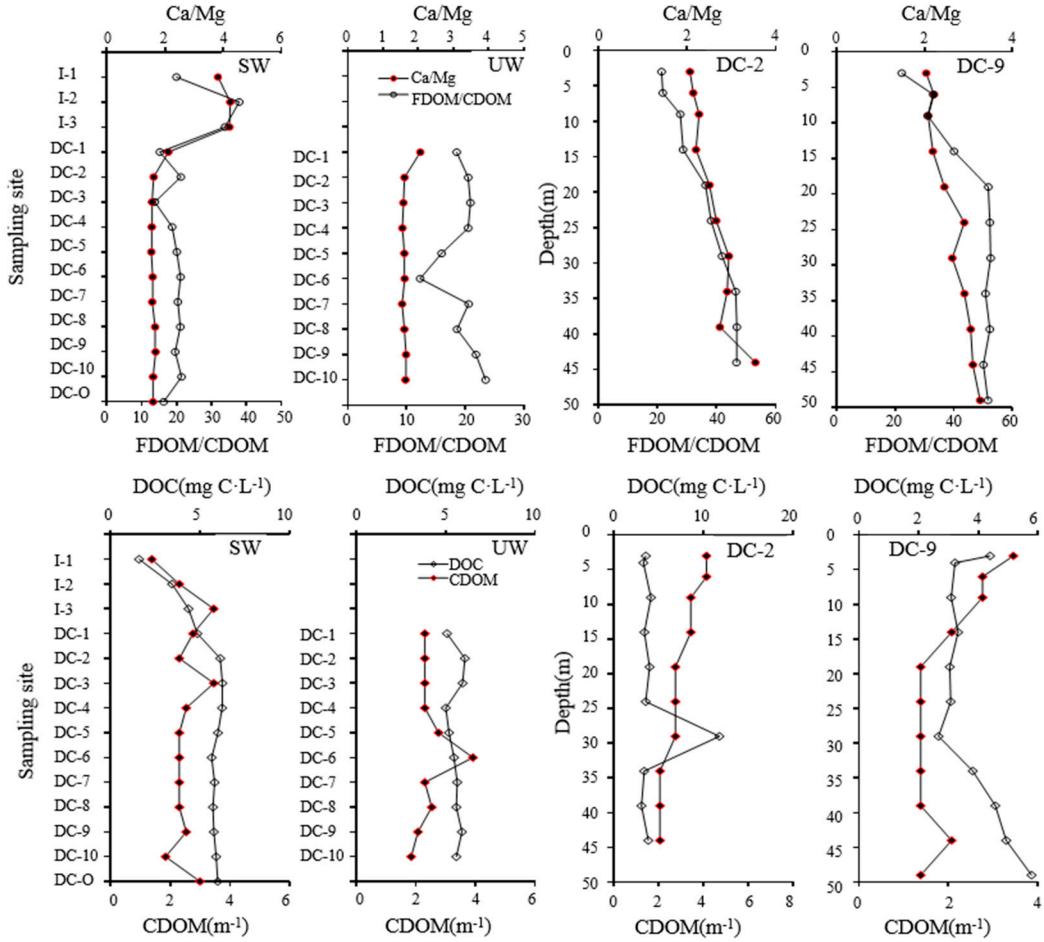

Figure 4. The variation trends of Ca/Mg and organic component (FDOM/CDOM) ratios in horizontal and vertical watercourses in Dianchi Lake. SW: surface water; UW: underlying water. For the sampling sites (I-1, I-2, I3, and DC1-10), see Figure 1. DOC: dissolved organic carbon; FDOM: fluorescent dissolved organic matter; CDOM: colored dissolved organic matter.

These ingredients were categorized into two primary components based on principal component analysis, and PC1 took a higher quotient. Closer to one on the vertical line indicates the stronger correlations with PC1 (Figure 5). Principal component analysis revealed that such nutrients as N species, Si and P, FDOM, and mineral elements were the principal ingredients in surface water.

Particulate degradation was associated with carbonatite and halide rock structures. The formation of encapsulation of bacterial/algal cells into mineral lattice or input from ground runoff resulted in a high score of PC1 and a low score of PC2 in surface water based on principal component analysis (Figure 5). DOC ranged from 5.01 to 6.08 in underlying water, with a highest value of 6.08 mg C·L^{-1} at site DC-2 and a minimum of 5.01 at DC-4. HCO_3^- and did not show any correlation to pH and DO; thus, it seemed that a series of biogeochemical processes of organic matter were irrelevant to mineral disintegration. As illustrated in Figure 5, PC1 was mainly composed of N, P, Si, and Ca/Mg in the underlying water, and they originated from disintegration of carbonatite minerals but significantly anti-correlated with SO_4^{2-} and Cl^-, fully demonstrating that S-/Cl-associated halide was transformed microbially into carbonatite or that mineralogical rearrangement happened. DOM therefore was produced and consumed during a series of complicated reactions.

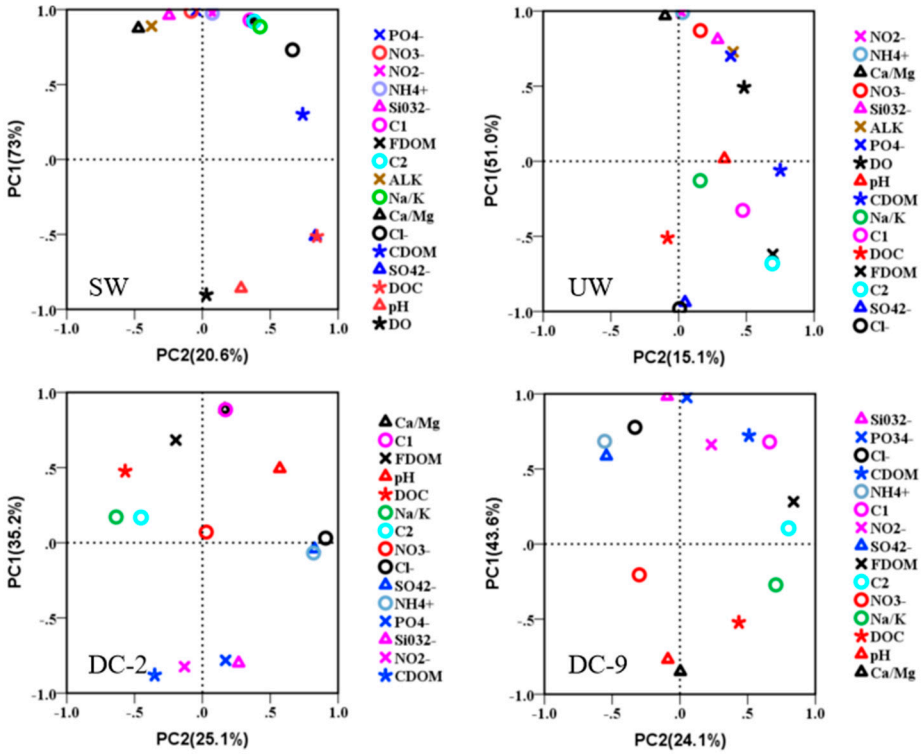

Figure 5. PC1 and PC2 loadings of DOM indices and environmental factors in surface (SW) and underlying (UW) pore waters at DC-2 and DC-9. PC1 and PC2 were obtained from principal component analysis. PC1: first primary component; PC2: second primary component.

In the pore water of site DC-2, positive correlations between DOC and the fluorescent intensity of the protein-like substance (protein-like intensity and DOC, $R^2 = 0.77$, $P \leq 0.01$) were observed, demonstrating that DOM was mainly the product of bacterial activities, and the vertical distribution of protein-like components manipulated the overall profile of DOM. DOC ranged from 3.1 to 11.81 mg C·L^{-1}, and it abruptly went up to 11.81 mg C·L^{-1} at 29 cm from 3.58 mg C·L^{-1} at 24 cm and remained almost unchanged at any other depths. Microbes were observed to bind sediment using extracellular polysaccharides and occurred in patchy distributions within sediments [43]. SiO_3^{2-}, NO_2^-, and PO_4^{3-} were observed as highest in 9 cm deposits on the surface with 20.52, 0.73, and 0.84 mg·L^{-1}, respectively. DOM formation and N, P, and Si mobilization in pore water referred to early diagenetic reactions mediated by bacteria [16] (Figure 5). Ratios of Ca/Mg showed the highest value yet of 3.54 at 44 cm depth and changed conversely to the above mentioned nutrients (Figure 5). Moreover, it showed that CDOM originated from encapsulation disintegration of POM-carbonatite with microbial mediation in terms of negative correlations between CDOM and ratios of Ca/Mg ($R^2 = -0.73$, $P \leq 0.01$). CDOM changed positively with Mg dissolution rate relative to that of Ca from mineral detritus and

had stronger affinity to Mg than Ca. NO_2^-, as the electron acceptor, probably played a particularly active role for FDOM production in that, when NO_2^- rose to a peak of 727.77 μg·L^{-1} at 6 cm depth, FDOM instead dropped to a trough of 90.76 QSU. Percentages of CDOM in DOC or FDOM in CDOM showed significantly negative or positive correlations to ratios of Ca/Mg. This result indicated that quotients of organic components in DOC were related to decomposition of POM, which was complexed or encapsulated into mineral particles.

DOC in pore water at DC-9 exhibited a profile decreasing in the upper layer and increasing in the deep layer, and the minimum was 2.67 mg C·L^{-1} at 29 cm. DOC gradually accumulated along the deposition column with attenuation of sulfate-reducing bacteria behaviors. The profile trends for quotas of FDOM in CDOM were just like those of dissolved Ca in Mg (FDOM/CDOM and Ca/Mg, $R^2 = 0.67$, $P \leq 0.01$), suggesting that the relative amount of fluorescent components in chromophores was closely associated with lattice structures of carbonatite minerals. In contrast to pore water at DC-2, PC1 of high score was negatively correlated to ratios of Ca/Mg, whereas it was positively correlated to PO_4^{3-}, SiO_3^{2-}, and CDOM (Figure 5). This result was attributed to the dynamics of P-, Si-consuming rate, and Ca-dissolving rate relative to Mg. P, Si, CDOM, and Ca/Mg were homologous from mineral disintegration during diagenesis [9,10,21]. Although values of Ca/Mg increased along the deposition column, the growth rate of ratios still remained unchanged or even slightly attenuated instead of increasing. Two slopes of regression equations in models of both growth rates were 0 and 0.03. Comparatively, the growth rates of CDOM and dissolved P and Si were significantly elevated (Figure 5). Thus, the analysis suggested that DOM in Dianchi Lake waters was correlated closely and significantly with water chemistry and nutrients.

3.4. Optical Characterization of DOM for Tracing Moieties Conversion in Dianchi Lake Waters

$SUVA_{254}$ was used to characterize the moieties of aromaticity and double-bond structures. $SUVA_{260}$ was indicative of hydrophobic moiety in DOM. Molecules of aromaticity and double-bond conformation constituted the primary part in hydrophobic fractions [44]. $E_{253/203}$ denoted a species of substituted groups and the degree of substitution on aromatic rings. Percentages of FDOM or CDOM in DOC varied identically to the parameters $SUVA_{254}$ and $SUVA_{260}$ ($R^2 = 0.92$, $P \leq 0.01$), whereas the percentages varied conversely to $E_{253/203}$ ($R^2 = -0.82$, $P \leq 0.01$). Percentages of these two moieties in DOM amounted to up to 31.65 QSU·L·(mg C)$^{-1}$, 0.87 L·m^{-1}·(mg C)$^{-1}$ at inlets. It suggested that the structures and the properties of DOM were regulated by the quotients of FDOM and CDOM in DOC. Aromaticity and hydrophobicity decreased with FDOM and CDOM percentages in attenuating DOM. $SUVA_{254}$ decreased quickly from 4.92 at inlets to 3.05 L·m^{-1} (mg C)$^{-1}$ at DC-2, whereas $E_{253/203}$ values increased initially from 0.01 at inlets to 0.13 at DC-2 and thereafter kept constant. Higher percentages simplified substituted groups on aromatic rings, aliphatic chains were considered the principal substituted types, and structures of DOM became firmer in the central water area compared to that at inlets. Aromaticity and hydrophobicity attenuated as HIX decreased (Figure 6), mainly due to biological activities being more frequent at the central lake region than at inlets from data of BIX. C1 of FDOM and CDOM did not originally correlate with each other, but their proportions in DOC varied identically ($R^2 = 0.74$, $P \leq 0.01$) with higher levels of 12.10 QSU·L·(mg C)$^{-1}$ and 0.87 L·m^{-1}·(mg C)$^{-1}$ at inlets, demonstrating that they were produced and accumulated in specific proportions. The proportions of C1/CDOM controlled the size of organic fractions (C1/CDOM and S_R, $R^2 = -0.76$, $P \leq 0.01$) that molecular weight was relatively lower than that of inlets. In Figure 7, PC1 was mainly represented by aromaticity and hydrophobicity of water, which was regulated by percentages of CDOM or even FDOM in DOC. S_R and $E_{253/203}$ values increased with these optical properties attenuated, and molecular weight of DOM and properties decreased, whereas molecular structure became firmer and less susceptible to be utilized by microbes from inlets to the central water area. DOM from fresh terrestrial plants/anthropogenic wastes should have had a high score of PC1 due to elevated proportions of CDOM in DOC at inlets but a low score of PC2 due to microbial humification by utilizing proteins in FDOM (Figure 7).

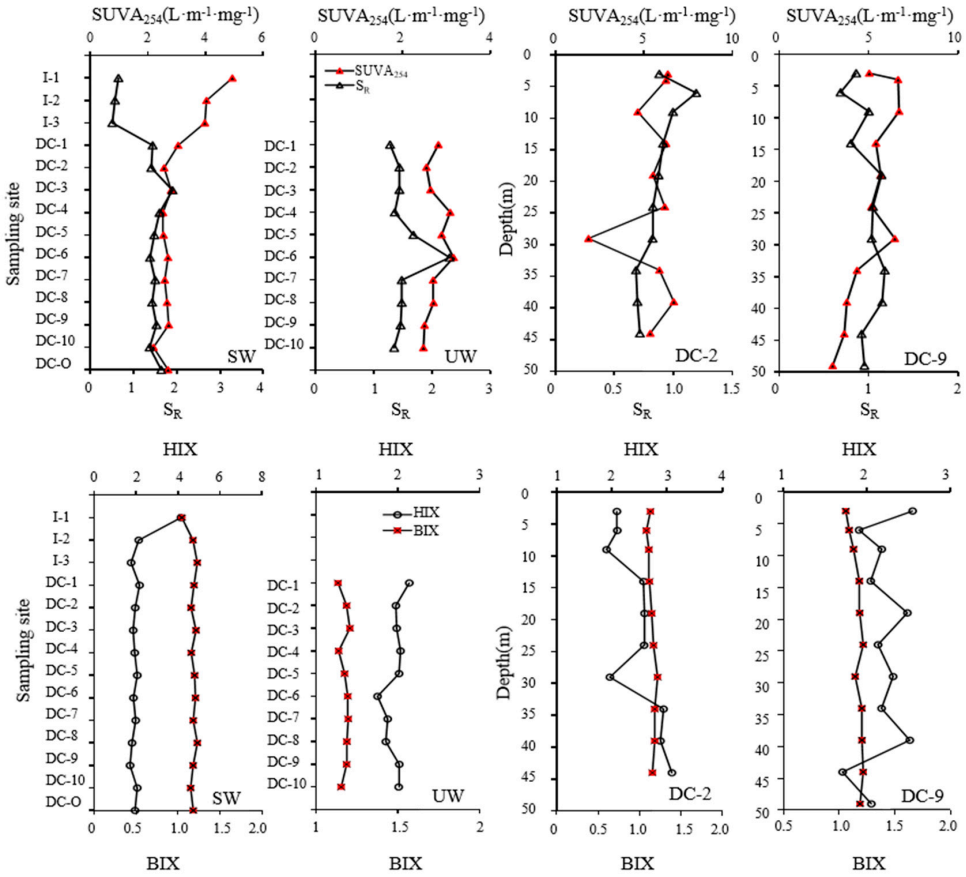

Figure 6. The characterization of aromaticity and molecular weight of DOM in horizontal and vertical watercourses in Dianchi Lake. S_R: the absorption spectral slope ratio. HIX: humification index. BIX: biological index.

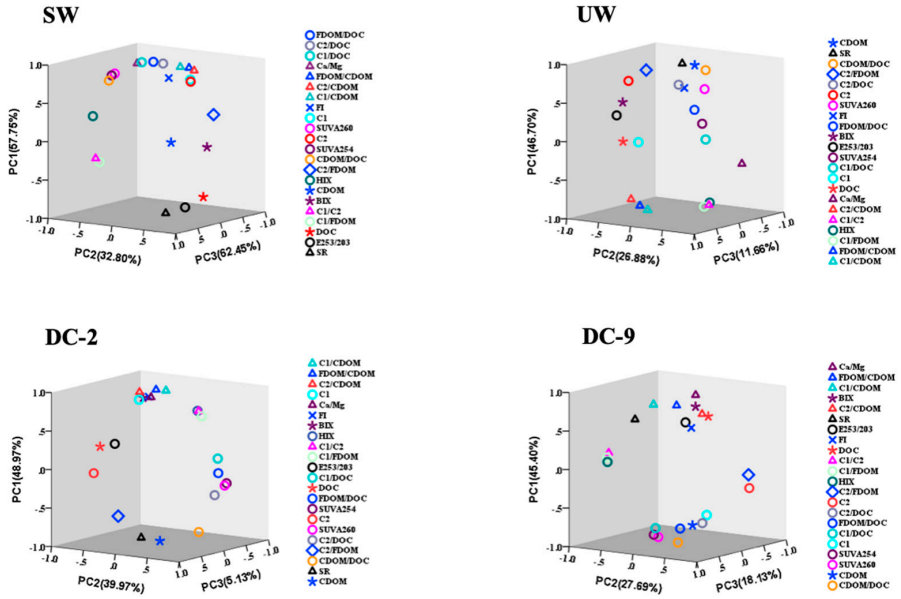

Figure 7. PC1, PC2, and PC3 loadings of optical indices and the relationship between organic components percentages and structures of DOM in surface (SW) and underlying (UW) water as well as pore water in sediments of DC-2 and DC-9. PC1, PC2, and PC3 were obtained from principal component analysis. PC1: first primary component; PC2: second primary component; PC3: third primary component.

$SUVA_{254}$ and $SUVA_{260}$ in underlying water were highest at site DC-6 with 3.16 and 2.99 L·(mg C·m)$^{-1}$, respectively, and abruptly dropped to minimums at DC-10 for $SUVA_{254}$ and $SUVA_{260}$ with 2.47 and 2.30 L·m^{-1}·(mg C)$^{-1}$. The aromaticity and the hydrophobicity of DOM were determined by the percentages of CDOM in DOC (CDOM/DOC and SUVA, $R^2 = 0.84$, $P \leq 0.01$). CDOM/DOC displayed an increasing-decreasing horizontal trend, and the highest value was 0.72 L·m^{-1}·(mg C)$^{-1}$ at DC-6. The S_R value exhibited a consistent trend with CDOM/DOC ($R^2 = 0.78$, $P \leq 0.01$) and the opposite trend with C1/CDOM ($R^2 = 0.78$, $P \leq 0.01$), expounding non-chromophores in DOM and the fluorophores in CDOM, which resulted in higher molecular weight. Then, bio-utilization of DOM reduced and humification elevated. PC1 had a high score, mainly due to CDOM percentages in DOC (specifically protein-like percentages in DOC). PC2 occupied the lower score precisely due to humification being decreased and fluorophores being bio-transformed into non-fluorophores [17,33].

$SUVA_{254}$ and $SUVA_{260}$ averaged 5.50 and 4.89 L·(mg C·m)$^{-1}$ in pore water at site DC-2, dropping dramatically to troughs at 29 cm sediment depth with 1.87 and 1.64 L·(mg C·m)$^{-1}$. SUVA values and FDOM/DOC had peak values at 39 cm with 6.69 and 5.79 L·m^{-1}·(mg C)$^{-1}$ and 38.9 QSU·L·(mg C)$^{-1}$. Percentages of FDOM in DOC had a similar profile to values of $SUVA_{254}$ and $SUVA_{260}$ ($R^2 = 0.92$, $P \leq 0.01$). The results indicated that fluorescent substances regulated properties of DOM greatly in biogeochemical processes; the larger percentages of fluorescent components in DOM resulted in the more stable properties of DOM. FDOM quotients in DOM regulated aromaticity and hydrophobicity of DOM, and the frequency of microbiota behavior was reflected in the percentages of fluorescent components in chromophores with the result that more frequent activities of microbiota resulted in higher percentages for FDOM in CDOM, especially percentages of C2 in CDOM (BIX and C2/CDOM, $R^2 = 0.8$, $P \leq 0.01$). It explained that microbiota behaviors were mainly reflected in the protein-like fluorescence in chromophores, and non-fluorescent fractions in CDOM were also transformed into fluorescent fractions with microbial mediation [2,12]. This result showed that humic substances originated in part from microbial activities, and protein-like fractions were indeed transformed into humic fractions from anti-correlations of quotient data for C1/FDOM and C2/FDOM. Meanwhile, non-chromophores in DOM were also bio-available from the data between the ratios of CDOM/DOC and BIX. Molecular weight of DOM increased gradually under intense metabolic behaviors of microbiota along the deposition column, and bio-aggregation was mainly low molecular weight reflected in percentages of FDOM in CDOM (specifically in quotients of C1/CDOM). Intense microbial metabolism resulted in molecular size shrinking within 6 cm of the surface layer sediments such that the S_R reached the peak value of 1.19 at 6 cm depth, and thereafter molecular weight started to grow (BIX and S_R, $R^2 = -0.65$, $P \leq 0.01$). PC1 for optical properties significantly correlated with FDOM percentages positively in DOC as well as hydrophobicity and aromaticity of DOM.

In the pore water of site DC-9, percentages of FDOM in DOC showed positive correlations to SUVA values, and aromaticity and hydrophobicity attenuated with decreasing quotients of fluorophores in DOC along the deposition column (FDOM/DOC and SUVA. $R^2 = 0.86$, $P \leq 0.01$) (Figure 7). In contrast to pore water at DC-2, $SUVA_{254}$ reached up to 6.47 at 30 cm deposition depth (Figure 6). BIX was regulated by ratios of FDOM/CDOM—specifically by quotients of C2/CDOM—which indicated that whatever the humic or the non-fluorophores' transformation to proteins in CDOM were, both provided abundant bioavailable fractions and contributed a great deal to bio-activities [17]. Meanwhile, transformation from chromophores of non-fluorescence emission to non-chromophores also resulted in more active biological behaviors (CDOM and BIX, $R^2 = -0.69$, $P \leq 0.01$). The molecular weight of DOM was mainly related to humic percentages in CDOM [16], demonstrating that the high molecular weights of non-fluorophores in CDOM were degraded along the deposition column, and humic-like DOM was mainly composed of low molecular weight components. PC1 was dominated primarily by CDOM percentage in DOC. When this proportion was elevated, aromaticity and hydrophobicity of DOM increased with it, as did molecular weight, whereas this high proportion for CDOM in DOC created low microbial-associated performances on surface sediment of 9 cm. Non-fluorescent fractions in CDOM and non-chromophores in DOC were both bio-available (Figure 7).

These optical indexes not only depicted the biogeochemical mobility and the transformation, they were also associated with lake eutrophication. Optical parameters were used to indicate the trophic state of the reservoir, and it was found that $SUVA_{254}$ and HIX had a good relationship with the modeled trophic state index. These optical indices reflected the trophic state of natural water [12]. HIX showed a converse trend to BIX in surface and underlying water ($R^2 = -0.76$, $P \leq 0.01$) in that they were regulated by C1/FDOM and C2/FDOM, and these two components were mutually converted. HIX in the underlying and the pore water at DC-2 also had a consistent relationship with molecular weight, and higher humification resulted in higher molecular weight (Figure 7). In effect, molecular weight increased with depth mainly due to bio-aggregation in pore water at DC-9. Percentages of CDOM in DOC played an important role in predominating aromaticity, hydrophobicity, and molecular weight except for the pore water at DC-2. Terrestrial aromaticity $SUVA_{254}$ was regulated by humic components in DOC except for the underlying water. Bio-activities in water above the deposition layer could intervene in the conversion of proteins and humic-like components in FDOM [11,17], which were observed from correlations between BIX and percentages of C2/FDOM, whereas bio-interventions in pore water were limited to conversions between proteins and humic-like substances, fluorophores, and non-fluorophores in CDOM [3,35]. Except for high bio-availability and intermolecular transformation, bio-activities (BIX) seemed to intervene in the production of cations (Ca/Mg) and organic ingredients (C2/CDOM) in pore water DC-2 and DC-9 (Figure 7). Molecular weights in water were regulated by percentages of C1 in CDOM. Generally, higher humic quotients in CDOM caused higher molecular weight, but pore water at DC-9 was an exception in that molecular weight decreased with increasing quotients C1/CDOM along the deposition column.

4. Conclusions

This study investigated the fluorescence of DOM, major ions, and nutrients in waters of Dianchi Lake in southwestern China. DOM in lake waters mainly derived from humic-like and protein-like components, especially in pore water. Aromaticity and hydrophobicity were regulated by percentages of chromophores and fluorophores of DOM. Nutrients acted not only as electron acceptors to oxidize OM but also as the products of mineral disintegration during metabolic behaviors. The different properties of organic moieties could be converted into each other except for direct biological assimilation and dissimilation. Mineral sources of organic components determined its properties, and normalizations of FDOM by CDOM or by DOC were closely related to mineral structures exampled as ratios Ca/Mg, and FDOM/CDOM was relevant to organic properties SUVA, HIX, BIX, and S_R. Organic molecules could be transformed or influenced by mineral structures and originated directly from disintegration, thus affecting the properties of molecules. However, there was no indication that DOM was related to mineral disintegration in the underlying water, mainly due to a series of complicated reactions during mineral structure rearrangement. The organic matter, the rocks, and the micro-organisms were connected intimately in lake sedimentation. Organic matter aggregation or adsorption onto the mineral surface is an important preservation approach other than complete initial encapsulation of living bacterial cells during deposition. The results in this study could provide insights into the transformation and the fate of DOM, water quality evolution, and the ecological significance of the aquatic environment in lake systems.

Author Contributions: M.X. and F.W. designed the research, M.X., Y.Y. and Z.H. conducted the field sampling, analyzed the samples, M.X. and Z.W. drafted the manuscript. All authors contributed to the results discussion and the manuscript modification.

Funding: This study was financially supported by National Natural Science Foundation of China (41373138) and Talent Introduction Project from Tianjin Normal University, China (5KGCC18002).

Acknowledgments: We thank Eileen Richardson from University of Glasgow for polishing the English text.

Conflicts of Interest: The authors declare no conflict of interest.

References

1. Thomas, J.D. The role of dissolved organic matter, particularly free amino acids and humic substances, in freshwater ecosystems. *Freshw. Biol.* **1997**, *38*, 1–36. [CrossRef]
2. Gao, Z.; Guéguen, C. Size distribution of absorbing and fluorescing DOM in Beaufort Sea, Canada Basin. *Deep Sea Res. Part I Oceanogr. Res. Pap.* **2017**, *121*, 30–37. [CrossRef]
3. Chen, B.; Huang, W.; Ma, S.; Feng, M.; Liu, C.; Gu, X.; Chen, K. Characterization of Chromophoric Dissolved Organic Matter in the Littoral Zones of Eutrophic Lakes Taihu and Hongze during the Algal Bloom Season. *Water* **2018**, *10*, 861. [CrossRef]
4. Kitis, M.; Karanfil, T.; Kilduff, J.E.; Wigton, A. The reactivity of natural organic matter to disinfection by-products formation and its relation to specific ultraviolet absorbance. *Water Sci. Technol.* **2001**, *43*, 9–16. [CrossRef] [PubMed]
5. Egeberg, P.K.; Alberts, J.J. Determination of hydrophobicity of NOM by RP-HPLC, and the effect of pH and ionic strength. *Water Res.* **2002**, *36*, 4997–5004. [CrossRef]
6. Fellman, J.B.; Hood, E.; Spencer, R.G. Fluorescence spectroscopy opens new windows into dissolved organic matter dynamics in freshwater ecosystems: A review. *Limnol. Oceanogr.* **2010**, *55*, 2452–2462. [CrossRef]
7. Li, S.; Zhang, J.; Mu, G.; Ju, H.; Wang, R.; Li, D.; Shabbir, A.H. Spatiotemporal Characterization of Chromophoric Dissolved Organic Matter (CDOM) and CDOM-DOC Relationships for Highly Polluted Rivers. *Water* **2016**, *8*, 399. [CrossRef]
8. Manenti, S.; Todeschini, S.; Collivignarelli, M.C.; Abbà, A. Integrated RTD—CFD Hydrodynamic Analysis for Performance Assessment of Activated Sludge Reactors. *Environ. Process.* **2018**, *5*, 23–42. [CrossRef]
9. Gu, B.; Schmitt, J.; Chen, Z.; Liang, L.; McCarthy, J.F. Adsorption and desorption of different organic matter fractions on iron oxide. *Geochim. Cosmochim. Acta* **1995**, *59*, 219–229. [CrossRef]
10. Chin, Y.P.; Traina, S.J.; Swank, C.R.; Backhus, D. Abundance and properties of dissolved organic matter in pore waters of a freshwater wetland. *Limnol. Oceanogr.* **1998**, *43*, 1287–1296. [CrossRef]
11. Coelho, C.; Heim, B.; Foerster, S.; Brosinsky, A.; Carlos de Araújo, J. In Situ and Satellite Observation of CDOM and Chlorophyll-a Dynamics in Small Water Surface Reservoirs in the Brazilian Semiarid Region. *Water* **2017**, *9*, 913. [CrossRef]
12. Shang, Y.; Song, K.; Jacinthe, P.A.; Wen, Z.; Lyu, L.; Fang, C.; Liu, G. Characterization of CDOM in reservoirs and its linkage to trophic status assessment across China using spectroscopic analysis. *J. Hydrol.* **2019**, *576*, 1–11. [CrossRef]
13. Thurman, E.M. Organic Geochemistry of Natural Waters. Springer Science & Business Media: Dordrecht, The Netherlands, 2012; Volume 2.
14. Twardowski, M.S.; Boss, E.; Sullivan, J.M.; Donaghay, P.L. Modeling the spectral shape of absorption by chromophoric dissolved organic matter. *Mar. Chem.* **2004**, *89*, 69–88. [CrossRef]
15. Burgos, W.D.; Pisutpaisal, N.; Tuntoolavest, M.; Chorover, J.; Unz, R.F. Biodegradation of 1-naphthol in the presence of humic acid. *Environ. Eng. Sci.* **2000**, *17*, 343–351. [CrossRef]
16. Santos, L.; Santos, E.B.H.; Dias, J.M.; Cunha, A.; Almeida, A. Photochemical and microbial alterations of DOM spectroscopic properties in the estuarine system Ria de Aveiro. *Photochem. Photobiol. Sci.* **2014**, *13*, 1146–1159. [CrossRef] [PubMed]
17. Helms, J.R.; Stubbins, A.; Ritchie, J.D.; Minor, E.C.; Kieber, D.J. Absorption spectral slopes and slope ratios as indicators of molecular weight, source and photobleaching of chromophoric dissolved organic matter. *Limnol. Oceanogr.* **2008**, *53*, 955–969. [CrossRef]
18. Weishaar, J.L.; Aiken, G.R.; Bergamaschi, B.A.; Fram, M.S.; Fujii, R.; Mopper, K. Evaluation of specific ultraviolet absorbance as an indicator of the chemical composition and reactivity of dissolved organic carbon. *Environ. Sci. Technol.* **2003**, *37*, 4702–4708. [CrossRef] [PubMed]
19. Mostofa, K.M.G.; Liu, C.Q.; Feng, X.B.; Yoshioka, T.; Vione, D.; Pan, X.L.; Wu, F.C. Complexation of Dissolved Organic Matter with Trace Metal Ions in Natural Waters. In *Photobiogeochemistry of Organic Matter*; Mostofa, K.M.G., Yoshioka, T., Mottaleb, M.A., Vione, D., Eds.; Springer: Heidelberg, Germany, 2013; pp. 769–849.
20. Sun, H.W.; Yan, Q.S. Influence of Fenton oxidation on soil organic matter and its sorption and desorption of pyrene. *J. Hazard. Mater.* **2007**, *144*, 164–170. [CrossRef] [PubMed]

21. He, W.; Lee, J.H.; Hur, J. Anthropogenic signature of sediment organic matter probed by UV–Visible and fluorescence spectroscopy and the association with heavy metal enrichment. *Chemosphere* **2016**, *150*, 184–193. [CrossRef]
22. Hou, G.; Song, L.; Liu, J.; Xiao, B.; Liu, Y. Modeling of cyanobacterial blooms in hypereutrophic Lake Dianchi, China. *J. Freshw. Ecol.* **2004**, *19*, 623–629. [CrossRef]
23. Gong, Z.J.; Li, Y.L.; Shen, J.; Xie, P. Diatom community succession in the recent history of a eutrophic Yunnan Plateau lake, Lake Dianchi, in subtropical China. *Limnology* **2009**, *10*, 247–253. [CrossRef]
24. Huang, B.; Wang, B.; Ren, D.; Jin, W.; Liu, J.; Peng, J.; Pan, X. Occurrence, removal and bioaccumulation of steroid estrogens in Dianchi Lake catchment, China. *Environ. Int.* **2013**, *59*, 262–273. [CrossRef] [PubMed]
25. Stedmon, C.A.; Markager, S.; Bro, R. Tracing dissolved organic matter in aquatic environments using a new approach to fluorescence spectroscopy. *Mar. Chem.* **2003**, *82*, 239–254. [CrossRef]
26. McKnight, D.M.; Boyer, E.W.; Westerhoff, P.K.; Doran, P.T.; Kulbe, T.; Andersen, D.T. Spectrofluorometric characterization of dissolved organic matter for indication of precursor organic material and aromaticity. *Limnol. Oceanogr.* **2001**, *46*, 38–48. [CrossRef]
27. Yang, K.; Yu, Z.; Luo, Y.; Yang, Y.; Zhao, L.; Zhou, X. Spatial and temporal variations in the relationship between lake water surface temperatures and water quality-A case study of Dianchi Lake. *Sci. Total Environ.* **2018**, *624*, 859–871. [CrossRef] [PubMed]
28. Zhong, J.; Li, S.L.; Liu, J.; Ding, H.; Sun, X.L.; Xu, S.; Wang, T.J.; Ellam, R.M.; Liu, C.Q. Climate variability controls on CO_2 consumption fluxes and carbon dynamics for monsoonal rivers: Evidence from Xijiang river, Southwest China. *J. Geophys. Res. Biogeosci.* **2018**, *123*, 2553–2567. [CrossRef]
29. Sundelin, B.; Eriksson, A.K. Mobility and bioavailability of trace metals in sulfidic coastal sediments. *Environ. Toxicol. Chem. Int. J.* **2001**, *20*, 748–756. [CrossRef]
30. Zhu, W.Z.; Zhang, H.H.; Zhang, J.; Yang, G.P. Seasonal variation in chromophoric dissolved organic matter and relationships among fluorescent components, absorption coefficients and dissolved organic carbon in the Bohai Sea, the Yellow Sea and the East China Sea. *J. Mar. Syst.* **2018**, *180*, 9–23. [CrossRef]
31. Huguet, A.; Vacher, L.; Relexans, S.; Saubusse, S.; Froidefond, J.M.; Parlanti, E. Properties of fluorescent dissolved organic matter in the Gironde Estuary. *Org. Geochem.* **2009**, *40*, 706–719. [CrossRef]
32. Coble, P.G. Characterization of marine and terrestrial DOM in seawater using excitation-emission matrix spectroscopy. *Mar. Chem.* **1996**, *51*, 325–346. [CrossRef]
33. He, X.S.; Xi, B.D.; Li, X.; Pan, H.W.; An, D.; Bai, S.G.; Cui, D.Y. Fluorescence excitation–emission matrix spectra coupled with parallel factor and regional integration analysis to characterize organic matter humification. *Chemosphere* **2013**, *93*, 2208–2215. [CrossRef] [PubMed]
34. Li, X.; Guo, H.; Zheng, H.; Xiu, W.; He, W.; Ding, Q. Roles of different molecular weights of dissolved organic matter in arsenic enrichment in groundwater: Evidences from ultrafiltration and EEM-PARAFAC. *Appl. Geochem.* **2019**, *104*, 124–134. [CrossRef]
35. Ishii, S.K.; Boyer, T.H. Behavior of reoccurring PARAFAC components in fluorescent dissolved organic matter in natural and engineered systems: A critical review. *Environ. Sci. Technol.* **2012**, *46*, 2006–2017. [CrossRef] [PubMed]
36. Jørgensen, L.; Stedmon, C.A.; Kragh, T.; Markager, S.; Middelboe, M.; Søndergaard, M. Global trends in the fluorescence characteristics and distribution of marine dissolved organic matter. *Mar. Chem.* **2011**, *126*, 139–148. [CrossRef]
37. Bridgeman, J.; Bieroza, M.; Baker, A. The application of fluorescence spectroscopy to organic matter characterization in drinking water treatment. *Rev. Environ. Sci. Bio Technol.* **2011**, *10*, 277–290. [CrossRef]
38. Wu, F.C.; Tanoue, E. Tryptophan in the sediments of lakes from Southwestern China Plateau. *Chem. Geol.* **2002**, *184*, 139–149. [CrossRef]
39. Azam, F.; Malfatti, F. Microbial structuring of marine ecosystems. *Nat. Rev. Microbiol.* **2007**, *5*, 782–791. [CrossRef] [PubMed]
40. Chen, J.; LeBoeuf, E.J.; Dai, S.; Gu, B. Fluorescence spectroscopic studies of natural organic matter fractions. *Chemosphere* **2003**, *50*, 639–647. [CrossRef]
41. Koopmans, G.F.; Groenenberg, J.E. Effects of soil oven-drying on concentrations and speciation of trace metals and dissolved organic matter in soil solution extracts of sandy soils. *Geoderma* **2011**, *161*, 147–158. [CrossRef]

42. Lu, Y.; Allen, H.E. Characterization of copper complexation with natural dissolved organic matter (DOM)—link to acidic moieties of DOM and competition by Ca and Mg. *Water Res.* **2002**, *36*, 5083–5101. [CrossRef]
43. Playter, T.; Konhauser, K.; Owttrim, G.; Hodgson, C.; Warchola, T.; Mloszewska, A.M.; Gingras, M. Microbe-clay interactions as a mechanism for the preservation of organic matter and trace metal biosignatures in black shales. *Chem. Geol.* **2017**, *459*, 75–90. [CrossRef]
44. Gur-Reznik, S.; Katz, I.; Dosoretz, C.G. Removal of dissolved organic matter by granular-activated carbon adsorption as a pretreatment to reverse osmosis of membrane bioreactor effluents. *Water Res.* **2008**, *42*, 1595–1605. [CrossRef] [PubMed]